UJEAS

UNIZIK JOURNAL OF ENGINEERING AND APPLIED SCIENCES

UNIZIK Journal of Engineering and Applied Sciences 3(1), March (2024), 416-429
Journal homepage: https://journals.unizik.edu.ng/index.php/ujeas
PRINT ISSN: 2992-4383 || ONLINE ISSN: 2992-4391

Adsorption and thermodynamic study of the inhibition of corrosion of zinc in HCl medium using N-[(4{[(Z)-phenylmethylidene]amino}phenyl)sulfonyl] acetamide

C. Ogueji [1*], M. C. Mbah[1], O. K. Amadi[2], Linus N. Okoro[1] and C. P. Okoli[1]
[1]Department of Chemistry, Alex Ekwueme Federal University, Ndufu-Alike, Ebonyi State, 482131, Nigeria
[2]Department of Chemistry, Michael Okpara University of Agriculture Umudike, Abia State, 440101, Nigeria
[*]Corresponding Author's E-mail: ogueji.chikezie@funai.edu.ng

Abstract
The inhibition and adsorption potential of Schiff's base, N-[(4{[(Z)-phenyl methylidene]amino}phenyl)sulfonyl]acetamide (PMAPSA) for zinc corrosion in HCl solution at different temperatures were studied using gravimetric method. The PMAPSA, uninhibited and inhibited zinc samples were characterized using the Fourier transform infra-red spectrum, X-ray diffraction and scanning electron microscope (SEM). The inhibitive effect of PMAPSA depend on the immersion period, PMAPSA concentration and temperature. The study revealed that the higher the PMAPSA concentration the lower the weight loss. The inhibitor, PMAPSA was found to exhibit a maximum inhibitive efficiency of 65.1 % at 0.5 g of PMAPSA and at 303 K. The activation energy of the inhibited corrosion reaction ranged from 9.72 kJ mol^{-1} to 11.24 kJ mol^{-1} with 10.39 kJ mol^{-1} (average) which is more than the 4.49 $kJmol^{-1}$ obtained for the uninhibited. Thermodynamic assessment of the corrosion process revealed that the PMAPSA adsorption on the zinc surface is endothermic and spontaneous. The uptake characteristic of PMAPSA was best described by Langmuir isotherm and this further buttressed the conclusion that the mode of adsorption of PMAPSA may have followed chemisorption mechanism.

Keywords: Corrosion inhibition; inhibitor; adsorption, thermodynamics

1. Introduction

Corrosion is the chemical or electrochemical attack that causes deterioration or degredation in the physical, metallurgical and mechanical attributes of engineering materials (Ofuyekpone et al., 2021). It is an afflicting problem associated with every use of metals. Zinc is one of the important metals used for various industrial applications. Zinc corrosion is often accelerated by both acidic and alkaline solutions due to its amphoteric nature (Abdallaha et al., 2016). Acidic solutions are commonly employed in various industries for acid cleaning, descaling, pickling process and so forth, because of this zinc metal will undergo rapid corrosion (Guruprasad et at., 2020). Metal corrosion is a constant and continuous problem, often difficult to eliminate completely because metals generally tend to move to its original state by corrosion process. Prevention would be more practical and achievable than complete elimination (Eddy and Ameh, 2021). The use of corrosion inhibitor is one of the effective and reliable methods of preventing and reducing the rate of metal corrosion (Chahul et al., 2018). A corrosion inhibitor is "a chemical substance which, when added at low concentration to the corrosive medium, slows or stops the corrosion process of a metal in contact with that medium (Ikeuba et al., 2015; Onwu et al., 2016; Ekuma et al., 2017, Vashi and Zele, 2021; Bilgic, 2022).

Studies have shown that organic compounds containing heteroatoms such as nitrogen, sulphur, phosphorus and oxygen with high electron density as well as those containing multiple bonds which are considered as adsorption

centres, are effective as corrosion inhibitor (Aloysius et al., 20117; Swetha et al., 2018). But the challenges of managing most of these organic inhibitors rest on their cost, toxicity, ease of availability, and eco-friendliness (Eddy and Ameh, 2021), these properties restrict its use to inhibit the metal corrosion (Pathak and Pratiksha, 2016). As a result, many researchers are focusing their efforts on replacing these toxic inhibitors with non-toxic and eco-friendly ones.

Schiff bases are the compounds containing azomethine group (-HC=N-) and could be considered as one of the most important types of organic inhibitors. This is as a result of the presence of C=N-group, p-electrons of aromatic rings and the heteroatoms (N, O, P and S) that may be attached within the molecule, easy to adsorb on the metal to form a protective film (Gupta, 2016). The π- bonds in their structures as well as heteroatoms and the lone pair of electrons on nitrogen in a compound have been reported to render a compound an efficient corrosion inhibitor for metals and alloys (Hegazy et al., 2014; Onwu et al., 2016; Ekuma et al., 2017). Schiff's basees have other advantages such as easiness to prepare, high purity, non-toxic (unlike other organic and inorganic inhibitors), environmentally friendly and interacts strongly with metal surfaces (Singh and Quraishi, 2016; Elaryian et al., 2022).

Several authors have investigated and reported the corrosion inhibition potentials of different Schiff bases as non-toxic and eco-friendly corrosion inhibitors. Schiff bases like (E)-3-(1- ((2-aminophenyl)imino)ethyl)-4-hydroxy-6-methyl-2H-pyran-2-one; (E)-3-(1-((3-aminophenyl)imino)ethyl)-4-hydroxy-6-methyl-2H-pyran-2-one, and (E)-3-(1-((4-aminophenyl)imino)ethyl)-4-hydroxy-6-methyl-2H-pyran-2-one (Nahlé et al., 2021); 3-((5-mercapto-1,3,4-thiadiazol-2-yl) imino)indolin-2-one (Betti et al., 2023); 2-amino-9-(1H-indol-3-yl)-4-(4-methoxyphenyl)-7-oxo-1,7-dihydropyrido[1,2-b][1,2,4]triazepine-3,8,10-tricarbonitrile and ethyl 2-amino-8,10-dicyano-9-(2-hydroxy3-methoxyphenyl)-4-(4-methoxyphenyl)-7-oxo-1,7-dihydropyrido[1,2-b][1,2,4]triazepine-3-carboxy late (Paul at et al., 2021) were reported as good corrosion inhibitors for mild steel in acid corrosive medium; 4-hydroxyl phenyl methylidene-2-(1-phenyl ethylidene) hydrazine carbothioamide and 4-hydroxy phenyl [methylidene] amino-3, 4-dimethyl-5-phenyl cyclo pent-2-en-1-one (Onwu et al., 2016; Ekuma et al., 2017); N,N'-bis-(1-hydroxyphenylimine)-2,5-thiophenedicarboxaldehyde (Abd El Wanees and Seda, 2019) have been reported as good corrosion inhibitors of zinc in acidic medium.

The Schiff's base, N-[(4{[(Z)-phenylmethylidene]amino}phenyl)sulfonyl] acetamide (PMAPSA) has not been tested or reported for corrosion inhibition of zinc in any medium. For the present work, our research group has carried out FT-IR spectroscopy, SEM studies, X-ray diffraction and weight loss studies of corrosion of zinc metal in the absence and presence of different concentrations of PMAPSA in 1 M HCl solution. The structure of N-[(4{[(Z)-phenylmethylidene]amino}phenyl)sulfonyl]acetamide (PMAPSA) is shown in Scheme 1.

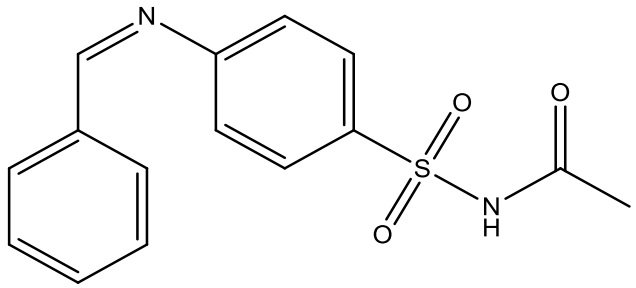

N-[(4{[(Z)-phenylmethylidene]amino}phenyl)sulfonyl]acetamide

Scheme 1: PMAPSA

2.0 Experimental

2.1 Materal collection and preparation

The Schiff's base, PMAPSA was synthesized through condensation reaction. This was carried out via condensation reaction, by refluxing sulphacetamide (2.14 g, 0.01 mol) with benzaldehyde (10 ml of 0.01 mol) in the presence of ethanol. Thin layer chromatography was used to monitor the reaction. The product was washed with 5:10 % ethylacetate-hexane mixture.

The zinc material employed in this work is composed of (wt %) Fe (0.002), Cd (0.001), Pb (0.001), Cu (0.0031) and Zn (99.99). The sheet material was press-cut into coupons of size 2 cm x 2 cm x 0.1 cm for each sheet. Each coupon was washed with ethanol, dried in acetone and stored in moisture free desiccators until the time of use (Ameh et al., 2012). A 1.0 M $HCl_{(aq)}$ was used for the gravimetric studies.

2.2. Characterisation

The composition of N-[(4{[(Z)-phenylmethylidene]amino}phenyl)sulfonyl] acetamide (PMAPSA) was analyzed using FTIR spectrum obtained from Frontier Perkin Elmer spectrophotometer in the range of 400 to 4000 cm^{-1}. X-ray diffraction pattern of PMAPSA was obtained using X-ray diffractometer (model: Bruker Smart 1000 CCD diffractometer). Scanning electron micrographs were obtained for the corroded coupons using scanning electron microscope, model SU9000. (Ma et al., 2015).

2.3 Gravimetric method

Weight loss analysis was carried out by dipping the previously weighed zinc coupons in 200 mL of the test solution (1 M HCl) in six different beakers at 303 K in a water bath containing different concentrations of PMAPSA (Onwu et al., 2016; Ekuma et al., 2017). The coupon was removed from the solution at the end of the exposure period (2 h), washed with 5% chromic acid solution containing 1% silver nitrate and 1% ammonium chloride to stop the corrosion reaction, rinsed in water and dried in acetone and reweighed (Onwu et al., 2016; Ekuma et al., 2017). This process was repeated at 313, 323 and 333 K. At 303 K, the experiment was repeated and the coupons were retrieved after every 1 h for 5 h (Eddy and Ameh, 2021). Equations 1, 2, 3 and 4, respectively were employed to calculate the weight loss, corrosion rate, degree of surface coverage and the inhibition efficiency (Eddy and Ameh, 2021).

$$\Delta W = Wo - W1 \quad (1)$$

$$\text{Corrosion rate} = \Delta W / At \quad (2)$$

$$\theta = \frac{CR_{un} - CR_{in}}{CR_{un}} \quad (3)$$

$$I.E\% = \frac{CR_{un} - CR_{in}}{CR_{un}}\ x\ 100 \quad (4)$$

Where W_o and W_1 are the initial and final weights of zinc coupons, CR_{in} and CR_{un} represents the PMAPSA-inhibited and uninhibited corrosion rates, t is the period of immersion and A is the specimen area (El-Haddadabd et al., 2019).

3.0 Results and Discussions

3.1. Characterization data

From the FTIR spectrum of PMAPSA (Figure 1), the following peaks represent the functional groups N-H (3139.17 cm^{-1}), C-H stretch (2919.85 cm^{-1}), C=N (1627.52 cm^{-1}), C=C (1585.95 and 1571.13 cm^{-1}), C-H (1492.23 and 1450.90 cm^{-1}), C-H bend (1339.45 and 1339.20 cm^{-1}), C-N (1261.17 cm^{-1}) and C-O (1029.53 cm^{-1}). The FTIR provides insight on the functional groups present in the compound and the formaton of the C=N-group at 1627.52 cm^{-1} (Omorogie et al., 2014; Nwanji et al., 2020;). PMAPSA is a white solid and the product yield is 72%.

From the XRD pattern obtained for PMAPSA (Figure 2), the peaks are sharp peaks which indicates that PMAPSA is crystalline in nature (Babalola et al., 2016).

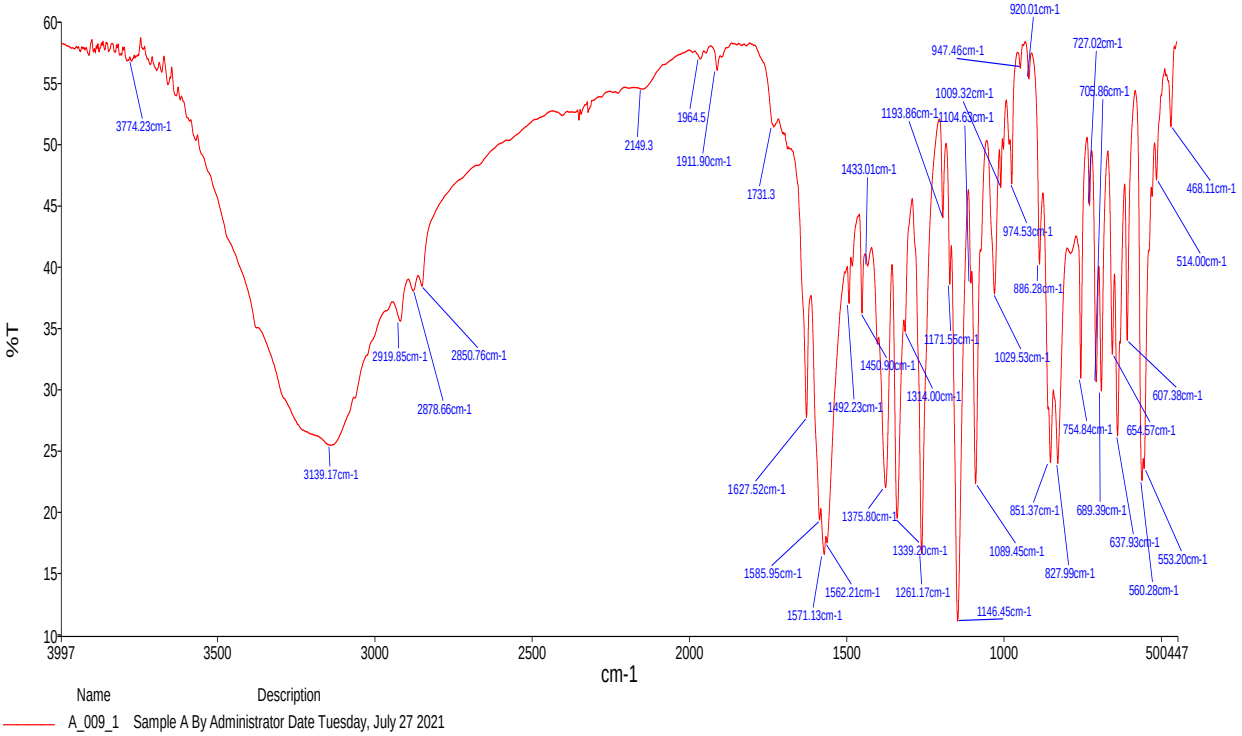

Fig.1: FTIR spectrum of PMAPSA

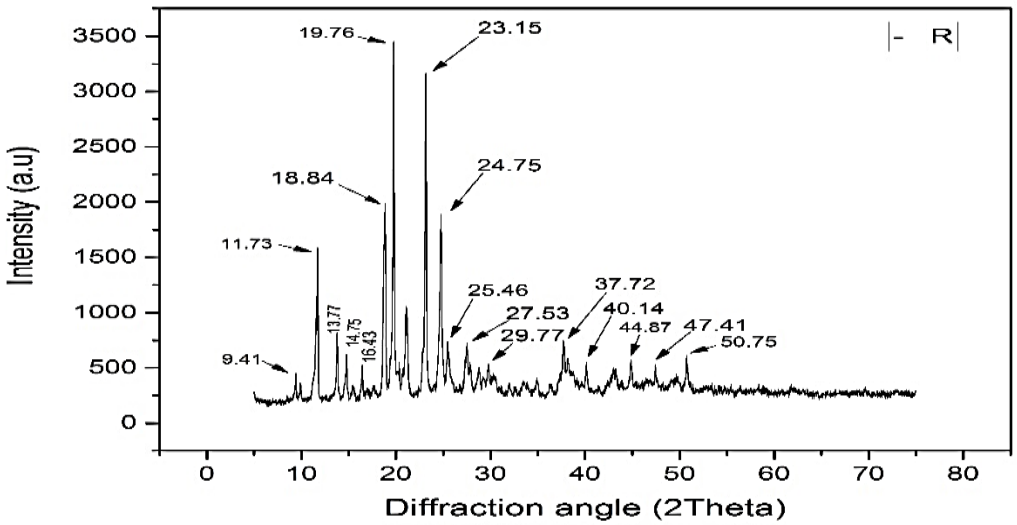

Fig.2: XRD pattern of PMAPSA

3.2 Effect of temperature and inhibitor concentration

At 303K, a weight loss of 0.2236g was obtained in 0.1 g of PMAPSA in 1 M $HCl_{(aq)}$, which decreased to 0.1908 g in 0.5 g of PMAPSA at same 303 K. It followed the same trend at 333 K, with weight loss of 0.3352g in 0.1 g of PMAPSA which decreased to 0.2724 in 0.5 g of PMAPSA.

Fig. 3 shows that there was a marked decrease in weight loss as PMAPSA concentration increased from 0.1 to 0.5g in 1 M $HCl_{(aq)}$. PMAPSA decelerated the corrosion reaction. However, higher weight loss of zinc in HCl solution at higher temperature, shows that increase in temperature increases the corrosion rate (Onwu et al., 2016; Ekuma et al., 2017; Burakov et al., 2018).

Inhibition efficiency of 47.4 % was obtained as the minimum in 0.1g of PMAPSA at 333K while 60.0% was the maximum in 0.5g of PMAPSA at 303K. Inhibition efficiency of PMAPSA increased with its concentration as shown in Fig. 4. Inhibition efficiency (%) of inhibitors increases with increase in inhibitor concentration (Ikeuba and Okafor, 2019). At 303K, a corrosion rate of 0.0140 $gcm^{-2}h^{-1}$ was obtained in 0.1g of PMAPSA and 0.0132 $gcm^{-1}h^{-1}$ in 0.5g of PMAPSA. At 333K, 0.0197 $gcm^{-2}h^{-1}$ was obtained in 0.1g of PMAPSA and 0.0189 $gcm^{-2}h^{-1}$ in 0.5 g of PMAPSA.

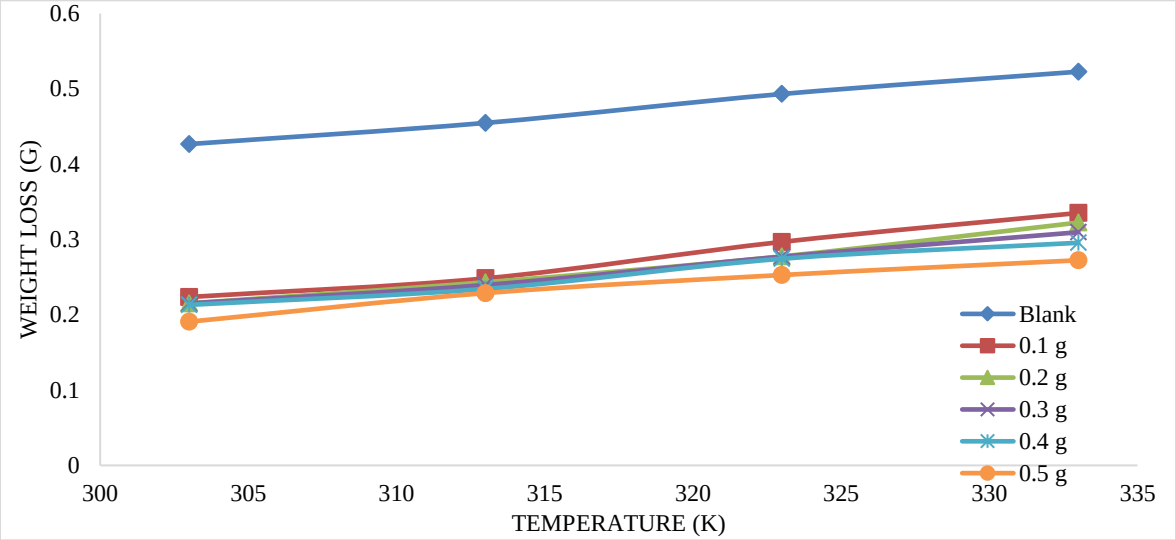

Fig.3: Plots of weight loss of zinc against temperature in 1 M of HCl at different PMAPSA dosage

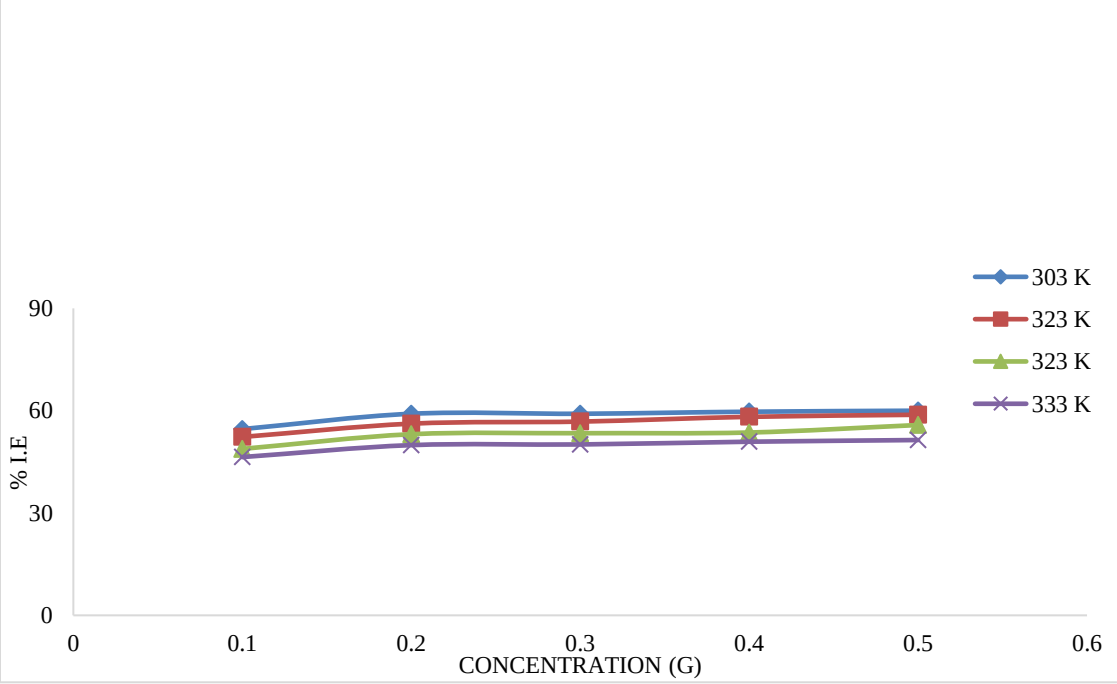

Fig.4: Plots of inhibition efficiency versus concentration of PMAPSA in 1 M of HCl at different temperature

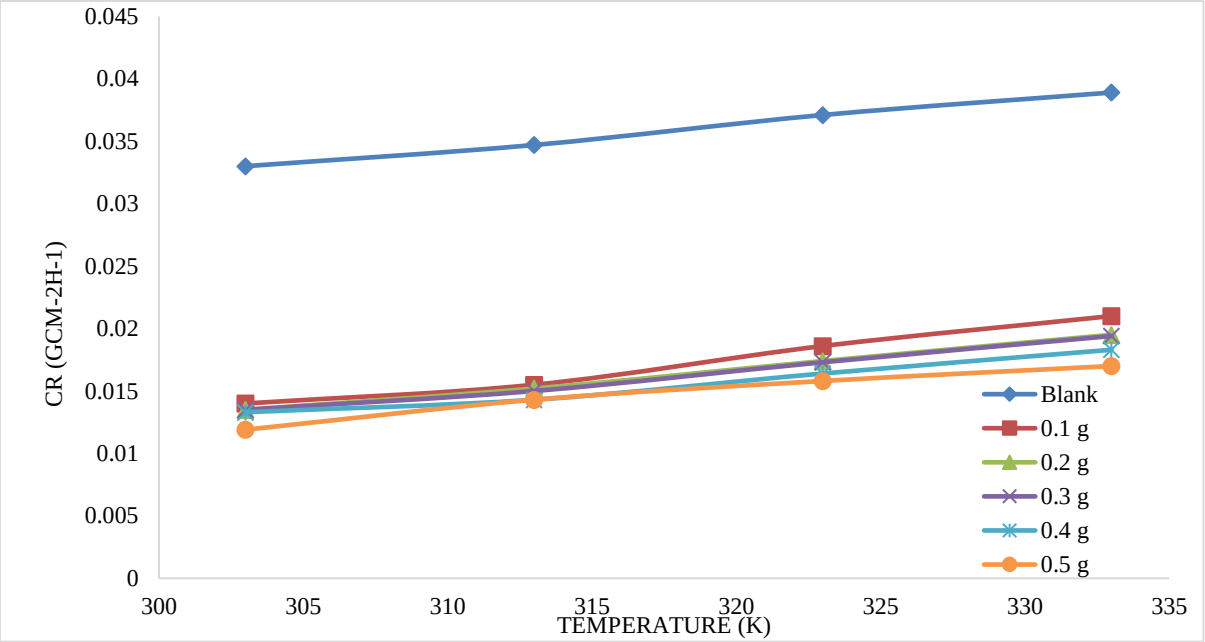

Fig.5: Plots of weight loss of zinc against temperature in 1 M of HCl at different PMAPSA dosage

3.3 Effect of immersion time

In 0.1g of PMAPSA, it was observed that the weight loss increased steadily from 0.1825g to 0.4053g as the immersion time increased from 1 to 5h respectively. But the weight loss decreased from 0.1825 to 0.1612g as PMAPSA concentration increased from 0.1 to 0.5g respectively. Fig. 6 shows that PMAPSA decelerated the rate of weight loss of the zinc in $HCl_{(aq)}$. It has been reported that weight loss of zinc increased with increase in the period of exposure and decreased with increase in the concentration of inhibitor (Okafor and Apebende, 2014).

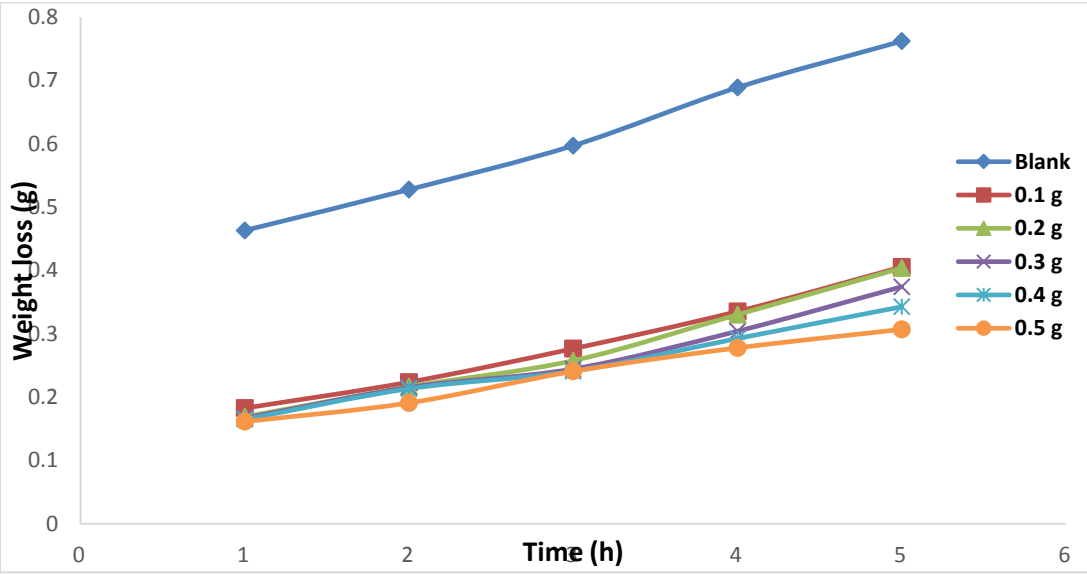

Fig.6: Plots of weight loss of zinc versus time in 1 M of HCl with PMAPSA at 303 K

The optimum inhibition efficiency of 65.1% was obtained in 0.5g of PMAPSA (Table 1), which decreased as the immersion time progressed.

Table 1: Inhibition efficiency, I.E (%) of zinc in 1 M of HCl at different time in PMAPSA at 303 K

Time (h)	0.1 g %I	0.2 g %I	0.3 g %I	0.4 g %I	0.5 g %I
1	60.6	63,3	64.0	64.4	65.1
2	55.6	59.5	59.1	59.7	60.0
3	53.6	56.8	59.0	59.5	59.8
4	51.4	52.1	55.8	57.7	59.5
5	46.8	47.1	48.3	55.0	58.4

3.4 Surface study by Scanning Electron (SEM)

Scanning electron micrograph of corroded zinc in 1 M $HCl_{(aq)}$ was obtained to study the surface morphology. The scanning electron micrographs of zinc in the absence and presence of PMAPSA are shown in Fig. 7(c) and 7(d) respectively. The observed flakes showing corrosion products in Fig. 7(c), implies that the zinc surface was seriously affected by corrosion. In the presence of PMAPSA, corroding effect on the zinc surface was seriously reduced (Figure 7d). Inhibitors form protective layer on metal surfaces (Guruprasad et al., 2020).

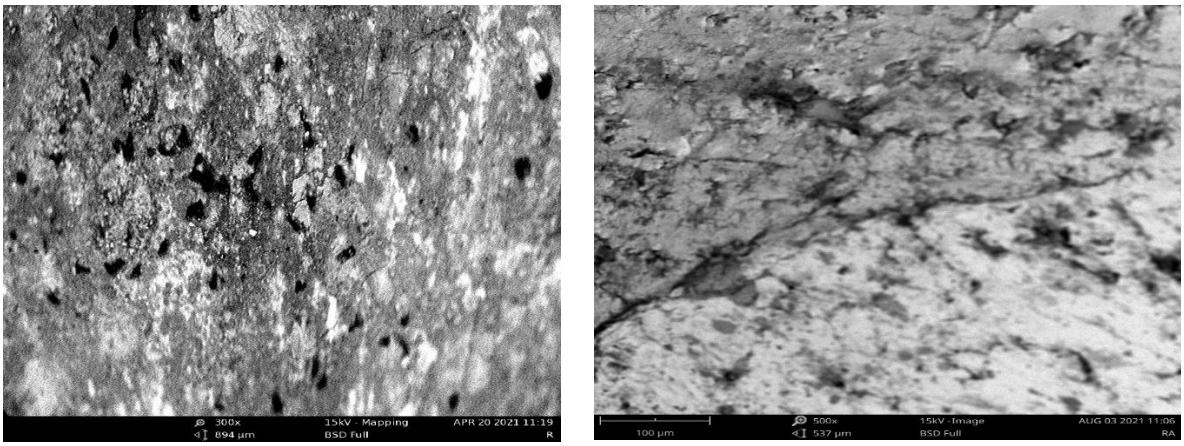

7(c) 7(d)

Fig.7: SEM for the uninhibited and PMAPSA-inhibited zinc

3.5 Adsorption consideration

Adsorption behaviour of PMAPSA on the surface of zinc was investigated using different adsorption isotherm models. PMAPSA adsorption data fitted best into Langmuir isotherm. Langmuir isotherm is expressed by equation (5), which simplifies to Equation (6) (Salman et al., 2019).

$$\frac{C}{\theta} = {}^{1}/_{K} + C \qquad (5)$$

$$\text{Log}\left(\frac{C}{\square}\right) = \log C - \log K \qquad (6)$$

Log(C/θ) against log C (from equation 6) should produce a linear graph if the Langmuir isotherm is obeyed (Onwu et al., 2016; Ekuma et al., 2017; Arthur, 2020). Figure 8 shows Langmuir plots for the inhibited corrosion reaction of zinc in 1 M $HCl_{(aq)}$. The high R^2 values (Table 2) ranging from 0.9996 to 1.0 implies that Langmuir gave the best description to the corrosion inhibition data. Langmuir isotherm and monolayer coverage implies chemisorption mechanism (Oyedeko et al., 2022).

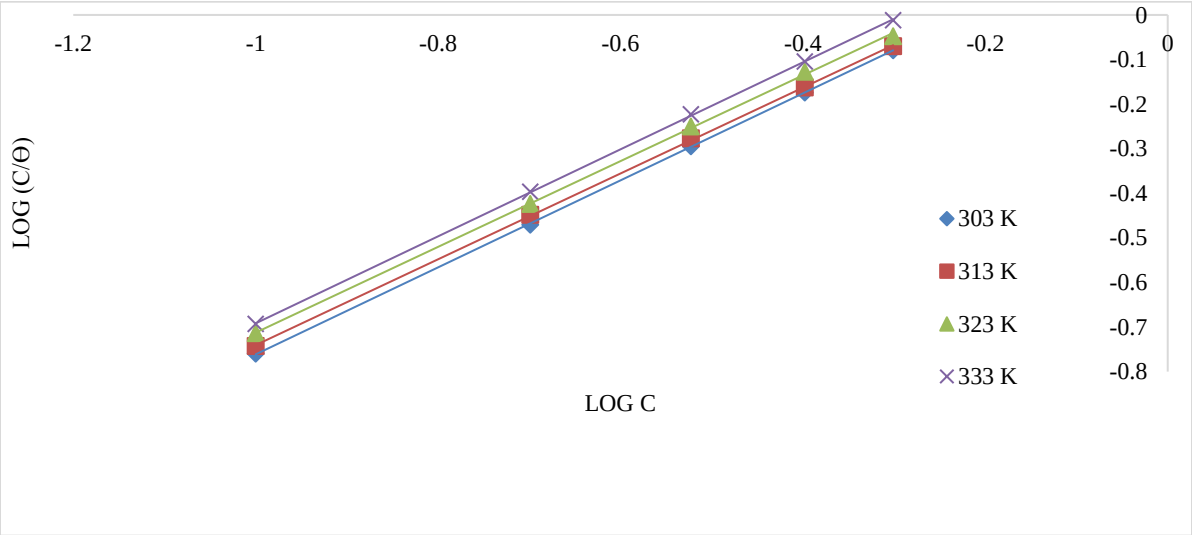

Fig.8: Langmuir plots for PMAPSA adsorption at different temperatures

Table 2: Langmuir isotherm parameters for PMAPSA uptake onto the surface

Temperature (K)	R^2	K_{ads}	Slope
303	1.0	1.6379	0.9756
313	0.9999	1.6665	0.9624
323	0.9996	1.7750	0.9617
333	0.9999	1.9231	0.9758

3.6 Kinetic and thermodynamic considerations

The experimental data were fitted into different kinetic order of reactions. The order and rate constants of PMAPSA-inhibited reaction were calculated and the results revealed that the corrosion reactions of zinc followed first order kinetics and similar results have been reported (Onwu et al., 2016; Ekuma et al., 2017). A first order equation is expressed according to equation (7), which on rearrangement and integration yields equation (8).

$$-d([A]_0 - y)/dt = k_1 t \quad (7)$$

$$-log\,([A]_o - y)/[A]_o = k_1 t/2.303 \quad (8)$$

Where $[A]_o$ and y are the concentrations of zinc at time t = 0 and at time, t. k_1 is the first order rate constant.
From equation (8), –log [weight loss] against time will give a linear graph (Onwu et al., 2016; Ekuma et al., 2017). Its slope is equivalent to -k_1 /2.303 and the half-lives of the uninhibited and PMAPSA-inhibited reactions were determined from equation (9) (Onwu et al., 2016; Ekuma et al., 2017).

$$t_{1/2} = 0.6931/k_1 \quad (9)$$

Figures 9 show kinetic plots for zinc corrosion in 1.0 M HCl at 303 K. The values of first-order rate constant (k_1) were determined from the slopes of the kinetic plots, and used to calculate values of half-life $t_{1/2}$ at different concentrations of PMAPSA using equation (9) (Nwigwe et al., 2019; Onwu et al., 2016; Ekuma et al., 2017) . The values of $t_{1/2}$ (Table 3) for the PMAPSA-inhibited reactions increased from 3.34 to 5.50 h, higher than 3.19 h obtained for the uninhibited. This implies that PMAPSA extended the half-life of the corrosion of zinc in the $HCl_{(aq)}$.

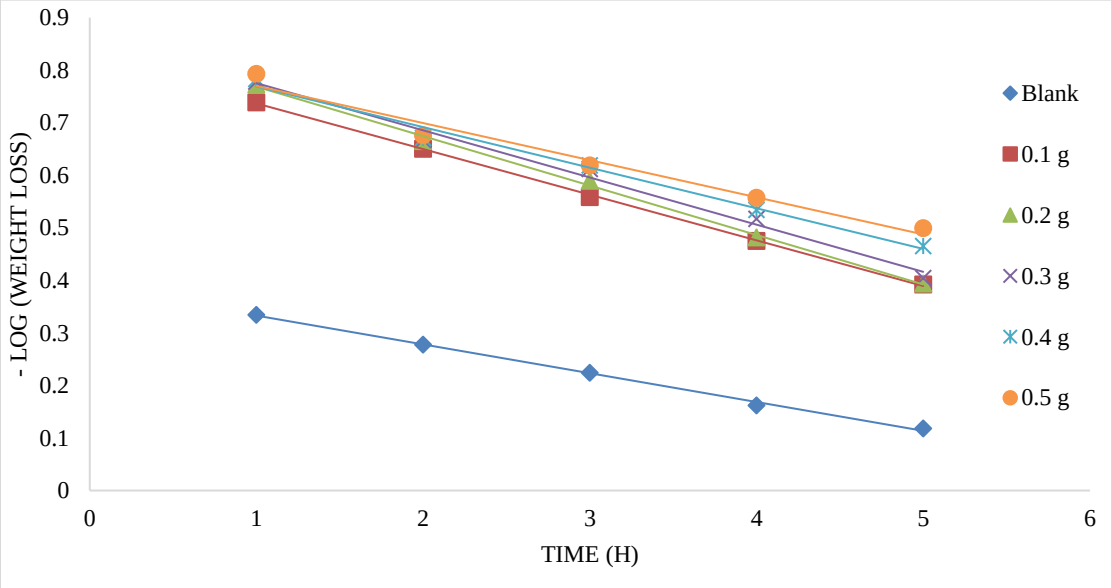

Fig.9: Kinetic plot for zinc corrosion in 1 M HCl

Table 3: Values of rate constant and half-life for zinc corrosion in 1.0 M HCl with PMAPSA at 303 K

	Blank	**0.1 g**	**0.2 g**	**0.3 g**	**0.4 g**	**.5 g**
k_1	0.217	0.207	0.200	0.178	0.163	0.126
$t_{\frac{1}{2}}(h)$	3.19	3.34	3.47	3.89	4.25	5.50

The activation energies for the zinc corrosion in HCl were determined using the Arrhenius relation expressed in equation (10) and on linearizing (10) equation (11) is obtained (Ikeuba et al., 2013).

$$CR = A \exp(-Ea/RT) \quad (10)$$

$$Log\ CR = \log A - {}^{Ea}/_{2.303\ RT} \quad (11)$$

where CR is the rate of corrosion, Ea is the activation energy of corrosion, A is the pre-exponential factor, R the gas constant and T the temperature (Gupta et al., 2016).

From equation (11), log CR against 1/T gives a linear plot and its slope equal to -Ea/2.303R (Ikeuba et al., 2015; Eddy and Ameh, 2021). Figure 10 shows the Arrhenius plot for the inhibition of zinc corrosion in 1 M HCl in different concentrations of PMAPSA. The calculated values of Ea (Table 4) from the slope for the inhibited, ranged from 9.72 kJ mol^{-1} – 11.24 kJ mol^{-1} with 10.39 kJ/mol (average) which is more than the 4.49 kJ/mol obtained for the uninhibited. This implies that the PMAPSA mitigated the zinc corrosion in $HCl_{(aq)}$.

The transition state relation (equation 12) was employed for the thermodynamic parameters determination and the free energy, ΔG from equation (10) (Ikeuba et al., 2015; Eddy and Ameh, 2021).

$$Log\left(\frac{CR}{T}\right) = log\frac{R}{Nh} + \frac{\Delta S}{2.303R} - {}^{\Delta H}/_{2.303RT} \quad (12)$$

$$\Delta G = \Delta H - T\Delta S \quad (13)$$

Where ΔH is the enthalpy of adsorption, ΔS is the entropy of adsorption, ΔG is Gibbs free energy, R is the gas constant, T is the temperature, N is the Avogadro's number while h is the Planck's constant.

From equation (12), log (CR/T) against 1/T gives a linear graph (Onwu et al., 2016; Ekuma et al., 2017). Its slope and intercept are equal to - ΔH/2.303R and log R/Nh + ΔS/2.303R respectively (Ikeuba et al., 2015; Elaryian et al., 2022). Figure 11 shows the Transition state plots and the thermodynamic values (Table 5) for the PMAPSA adsorption onto the surface.

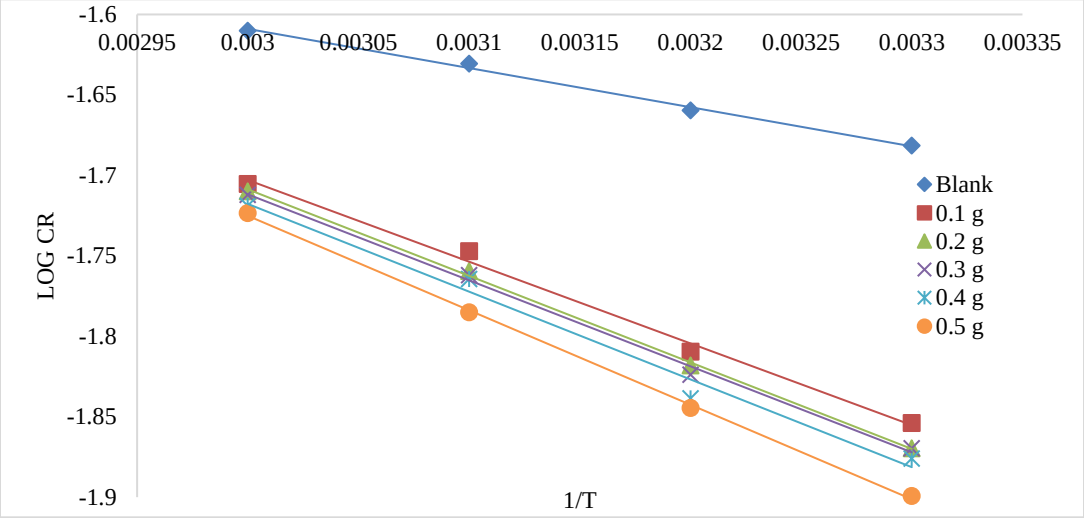

Fig.10: Arrhenius plot for the corrosion inhibition of zinc in 1 M of HCl

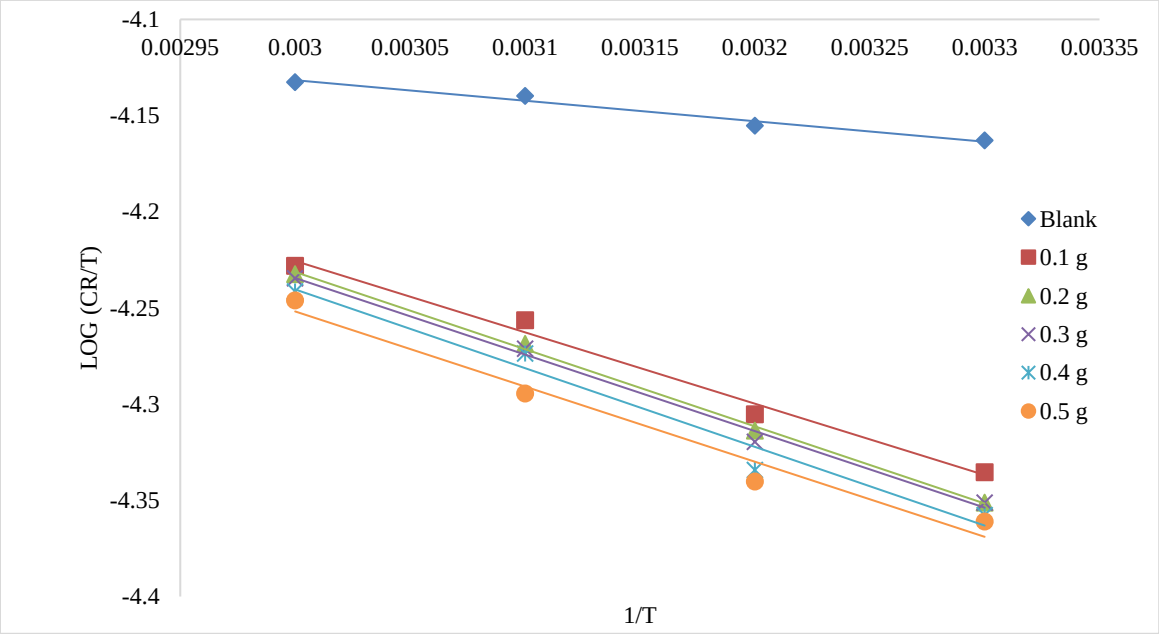

Fig.11: Transition state plot for the inhibition of zinc corrosion in 1 M of HCl

Table 4: Thermodynamic parameters for the PMAPSA uptake at different temperatures (in kJ/mol)

Conc. (g)	E_a	ΔH	ΔS	ΔG	ΔG	ΔG	ΔG
				303 K	313 K	323 K	333 K
0.0	4.49	2.041	0.155	-44.92	-46.47	-48.02	-49.57
01	9.72	7.100	0.164	-42.59	-44.23	-45.87	-47.51
0.2	10.30	7.680	0.166	-42.62	-44.28	-45.94	-47.60
0.3	10.23	7.617	0.165	-42.38	-44.03	-45.68	-47.33
0.4	10.44	7.833	0.166	-42.47	-44.13	-45.79	-47.45
0.5	11.24	7.477	0.165	-42.52	-4417	-45.82	-47.47

From Table 5, the calculated values of ΔH ranged from 7.100 kJ/mol to 7.833 kJ/mol with 7.541 kJ mol^{-1} (average) for the PMAPSA-inhibited reaction. The positive values of ΔH indicates that the adsorption of an inhibitor on a metal surface is endothermic in nature (Zhou et al., 2015; Gupta et al., 2016; Jagadeesan et al., 2016; Monk et al., 2021). The ΔS values (Table 5) were positive and ranged from 0.164 kJ/mol to 0.166 kJ/mol. The positive values of ΔS may suggest some structural rearrangement of the adsorbed PMAPSA compound upon inhibition and further revealed that the freedom of the inhibitor is not totally restricted even at the zinc surface (Ekuma et al., 2017). The determined values of ΔG ranged from -42.59 to -42.52 kJ mol^{-1} at 303 K, -44.23 to -4417 kJ mol^{-1} at 313 K, -45.87 to -45.82 kJ mol^{-1} at 323 K and -47.51 to -47.47 kJ mol^{-1} for the PMAPSA-inhibited reaction. Negative values of ΔG implies that the inhibitor adsorption onto the metal surface is spontaneous (Zhou et al., 2015; Gupta et al., 2016; Jagadeesan et al., 2016; Monk et al., 2021). The ΔG values for the PMAPSA inhibited reaction were above -40 kj/mol. It has been reported that ΔG values above the threshold value of -40 KJ/mol implies chemisorption (Abdallah et al., 2016).

4.0. Conclusion

The successful synthesis of the Schiff base, PMAPSA was done and its corrosion inhibition potential was tested in 1 M HCl solution at different temperatures using the weight-loss method.

The following conclusions are drawn from the results obtained for this study:

i. The Schiff base, PMAPSA was able to inhibit the corrosion of zinc in hydrochloric acid solution to a significant extent, with a maximum inhibition efficiency of 65.1 % in 0.5 g of PMAPSA at 303 K.

ii. The adsorption equilibrium constants values suggest that PMAPSA particles are chemically adsorbed and weakly bind to zinc surface, as the inhibiting performance increases with rising PMAPSA concentration and reduces with increasing temperature.

iii. The adsorption isotherm data fitted well into the Langmuir isotherm which suggests chemisorption interaction between the PMAPSA molecules and the zinc surface, since the calculated $\Delta Gads$ values for the inhibited reactions were between the range of −42.52 to −49.57 kJ/mol.

iv. Thermodynamic analysis showed that the adsorption was spontaneous, endothermic process.

v. In addition, the SEM images show that the PMAPSA prevents the metal surface from corrosive attack.

vi. The results of this study, shows that PMAPSA can be gainfully applied by researchers in corrosion field against corrosion attack on metallic materials.

5.0 Recommendation

It is recommended that more research be carried out using PMAPSA as a corrosion inhibitor for zinc and other metals in different acidic media.

Funding

This research received no external funding.

.

Acknowledgements

The authors of this research paper are grateful to the colleagues in the Department of Chemistry, Michael Okpara University, Umudike, Abia State, Nigeria and as well as to the colleagues in the Department of Chemistry, Alex Ekwueme Federal University Ndufu-Alike, Ebonyi State, Nigeria for their encouragement and support respectively.

References

Abdallaha, M., Zaafaranya, I.A., AL-Jahdalya, B.A., 2016. Corrosion Inhibition of Zinc in Hydrochloric Acid using some Antibiotic Drugs. J. Mater. Environ. Sci. 7 (4): 1107-1118.

Aloysius, A., Ramanathan, R., Christy, A., Anthony, N., 2017. Experimental and theoretical study of D-biotin as green corrosion inhibitors on the corrosion inhibition of carbon steel in chloride ion environment. Int. J. ChemTech Res. 10(10), 361-376.

Arthur. D.E., 2020. Computational and experimental study on corrosion inhibition potential of the synergistic 1:1 combination of Arabic and cashew gums on mild steel. Petroleum Research 5(2): DOI: 10.1016/j.ptlrs.2020.01.002

Babalola, J.O., Koiki, B.A., Eniayewu, Y., Salimonu, A., Olowoyo, J.O., Oninla, V.O., Alabi, H.A., Ofomaja, A.E., Omorogie, M.O., 2016. Adsorption efficacy of Cedrela odorata seed waste for dyes: nonlinear fractal kinetics and nonlinear equilibrium studies, J. Environ. Chem. Eng. 4 (2016) 3527–3536 https://doi.org/10.1016/j.jece.2016.07. 027.

Baijayantimala, S., Abrar, K., Priti, S., Vaibhav, S.M., Andrea, A., Krishnak, C., Venkata, M.V., Simone, C., Claudiu, S., Mohammed, A., 2022. Design, synthesis and biological assessment of Rhodanine-liked benzene sulfonamide derivatives as selective and potent human carbonic anhydrase inhibitors. *Molecules*, 27, 8028.

Betti, N.,.Al-Amiery, A., KhalidAl-Azzawi, W., Isahak, W,N., 2023. Corrosion inhibition properties of schif base derivative against mild steel in HCl environment complemented with DFT investigations. (2023) 13:8979. https://doi.org/10.1038/s41598-023-36064-w

Bilgiç, S., 2022. Plant extracts as corrosion inhibitors for mild steel in H2SO4 and H3PO4 media – Review II. Int J Corros Scale Inhib., 11(1), pp. 1–42. doi: 10.17675/2305-6894-2022-11-1-1.

Burakov, A.E., Galunin, E.V., Burakova, I.V., Kucherova, A.E., Agarwal, S., Tkachev, A.G., Gupta, V.K., 2018. Ecotoxicology and environmental safety adsorption of heavy metals on conventional and nanostructured materials for wastewater treatment purposes: a review, Ecotoxicol. Environ. Saf. 148 :702–712 https:// doi.org/10.1016/j.ecoenv.2017.11.034.

Chahul, H.F., Ndukwe, G.I., Ogwu, D.O., 2018. A thermometric study on the kinetics of the acid dissolution of aluminium in the presence of Napoleonaea imperialis seeds extract and iodide ions, Ovidius University Annals of Chemistry, 29(2): 103-109.

Eddy, N.O. and Ameh, P.O. 2021. Computational and experimental study on Tapinanthus bangwensis leaves as corrosion inhibitor for mild steel and Al in 0.1 M HCl. Current Topics in Electrochemistry Vol. 23, 2021.

Ekuma, F.K., Ogueji, C., Okoyeagu, A., 2017. Zinc corrosion inhibition by 4-hydroxyl phenyl methylidene-2-(1-phenyl ethylidene) hydrazine carbothioamide (4-HPMHC) and 4-hydroxy phenyl [methylidene] amino-3, 4- dimethyl-5-phenyl cyclo pent-2-en-1-one (4-HPMCP). J. Chem. Soc. Nigeria, 42(2): 5-10.

Elaryian, H.M., Bedair, M.A., Bedair, A.H., Aboushahba, R.M., Fouda, A.S., 2022. Synthesis, characterization of novel coumarin dyes as corrosion inhibitors for mild steel in acidic environment: Experimental, theoretical, and biological studies. Journal of Molecular Liquids, 346 https://doi.org/10.1016/j.molliq.2021.118310.

El-Haddadabd, M.N., Fouda, A.S., Hassan, A.F., 2019. Data from Chemical, electrochemical and quantum chemical studies for interaction between Cephapirin drug as an eco-Friendly corrosion inhibitor and carbon steel surface in acidic medium, 22: 100251 DOI: 10.1016/j.cdc.2019.100251.

Gupta, N. K.; Verma, C.; Quraishi, M. A.; Mukherjee, A. K., 2016. Schiff's Bases Derived from l-lysine and Aromatic Aldehydes as Green Corrosion Inhibitors for Mild Steel: Experimental and Theoretical Studies. J. Mol. Liq. 2016, 215, 47–57. DOI: 10.1016/j.molliq.2015.12.027.

Gupta, V.K., Carrott, P.J.M., Singh, R., Chaudhary, M., Kushwaha, S., 2016. Bioresource Technology Cellulose: a review as natural, modified and activated carbon adsorbent. Bioresour. Technol. 216:1066-1076 https://doi.org/10.1016/j. biortech.2016.05.106.

Guruprasada, A.M., Sachinb, H.P., Swethab, G.A., Prasannad, B.M., 2020. Corrosion inhibition of zinc in 0.1 M hydrochloric acid medium with clotrimazole: Experimental, theoretical and quantum studies. Surfaces and Interfaces, 19 (2020) 100478. https://doi.org/10.1016/j.surfin.2020.100478

Hegazy, M.A., Abdallah, M., Awad, M.K., Rezk, M., 2014. Part I: Experimental Results, Corros. Sci., 81: 54.

Ikeuba, A.I., Ita, B.I., Etiuma, R.A., Bassey, V.M., Ugi, B.U., Kporokpo, E.B., 2015. Green Corrosion Inhibitors for Mild Steel in H_2SO_4 Solution: Flavonoids of Gongronema latifolium. Chemical and Process Engineering Research, 34: 2224-7467.

Ikeuba, A.I., Okafor, P.C., 2019. Green corrosion protection for mild steel in acidic media: saponins and crude extracts of Gongronema latifolium. Pigment & Resin Technology, 48(1):57-64.

Jagadeesan, S., Sowmiya, M., Sounthari, P., Parameswari, K., Chitra, S., Senthilkumar, K., 2016. N-heterocycles as corrosion inhibitors for mild steel in acid medium, Journal of Molecular Liquids, 216:42-52.

Kadhum, A.H, Mohamad, A.B., Hammed, L.A., Al-Amiery, A.A., San, N.H., Musa, A.Y., 2014. Inhibition of Mild Steel Corrosion in Hydrochloric Acid Solution by New Coumarin. Material, 7 4335-4348, doi:10.3390/ma7064335.

Ma, J., Zhou, L., Dan, W., Zhang, H., Shao, Y., Bao, C., Jing, L., 2015. Novel magnetic porous carbon spheres derived from chelating resin as a heterogeneous Fenton catalyst for the removal of methylene blue from aqueous solution. J. Colloid Interface Sci 446:298–306. https://doi.org/10.1016/j.jcis.2015.01.036.

Nahlé, A., El Azzouzi, M., Aouniti, A., Abrigach, F., Djedouani, A., Benhiba, F., Touzani, R., Warad, I., Obot, I.B., Zarrouk, A., Hammouti, B., 2021. Experimental, Quantum Chemical and Monte Carlo Simulation Studies on the Corrosion Inhibition of Mild Steel by Three New Schiff Base Derivatives. Portugaliae Electrochimica Acta 39 (2021) 293-321.

Nwanji, O.L., Omorogiec, M.O., Olowoyob, J.O., Babalola, J.O., 2020. Remediation of industrial dye by Fenton-activated biogenic waste. Surfaces and Interfaces, 20(2020) 100555. https://doi.org/10.1016/j.surfin.2020.100555

Nwigwe, U., Mbam, S., & Umunakwe, R. 2019. Evaluation of Carica papaya leaf extract as a bio-corrosion inhibitor for mild steel applications in a marine environment. Mater Res Express., 6(10), pp. 1-13. doi: 10.1088/2053- 1591/ab3ff6.

Ofuyekpone, O.D., Utub, O.G., Onyekp, B.O., 2021. Corrosion inhibition for alloy 304L (UNS S30403) in H2SO4 1M solution by Centrosema pubescens leaves extract. Applied Surface Science Advances, 3(2021) 100061. https://doi.org/10.1016/j.apsadv.2021.100061

Okafor, P.C., Apebende, E.A., 2014. Corrosion inhibition characteristics of Thymus Vulgaris, Xylopia aethiopica and Zingiberofficinale extracts on mild steel in sulphuric acid solutions. Pigments and Resin Technology, 43(6):357 - 364.

Omorogie, M.O., Babalola, J.O., Unuabonah, E.I., Gong, J.R., 2014. Hybrid materials from agro-waste and nanoparticles: implications on the kinetics of the adsorption of inorganic pollutants. Environ Technol, 35(5):611–619, https://doi.org/10.1080/09593330.2013. 839747.

Omorogie, M.O., Babalola, J.O., Unuabonah, E.I., Gong, J.R., 2014. Solid phase extraction of hazardous metals from aqua system by nanoparticle-modified agrowaste composite adsorbents. J Environ Chem Eng, 2(1):675–684.

Onwu, F.K., Ogueji, C., Mgbemena, N.M., 2016. Inhibition of Corrosion of Zinc in H_2SO_4 Medium by the Schiff Base, 4-Hydroxy Phenyl Methylidene-2-(l-Phenyl Ethylidene) Hydrazine Carbothioamide (4-HPMHC). DerChemica Sinica, 7(4): 13-20.

Oyedeko, K., Lasisi, M., & Akinyanju, A. 2022. Study of Blend of Extracts from Bitter Leaf (Vernonia Amygdalina) Leaves and Banana (Musa Acuminata) Stem as Corrosion Inhibitor of Mild steel in Acidic Medium. Eur J Eng Technol Res., 7(1), pp. 1–9.

Pathak, R.K., Pratiksha M., 2016. Drugs as corrosion inhibitors: a review. J. Sci. Res. 5(4), 671-677.

Paul, P.K., Mehta, R.K., Yadav, M., Obot, I.B., 2021. Theoretical, electrochemical and computational inspection for anti-corrosion activity of triazepine derivatives on mild steel in HCl medium. Journal of Molecular Liquids. https://doi.org/10.1016/j.molliq.2021.118075

Salman, T. et al., 2019. Novel ecofriendly corrosion inhibition of mild steel in strong acid environment: Adsorption studies and thermal effects. Int J Corros Scale Inhib., 8(4), pp. 1123–1137. doi: 10.17675/2305-6894-2019-8-4-19.

Shaban, S., Abdelrhman, I., Mahmoud, M., El-Sukkary, A., El-Awady, M.Y., 2014. Inhibition of mild steel corrosion in acidic medium by some cationic surfactants. Journal of Molecular Liquids 203(5) DOI: 10.1016/j.molliq.2014.12.033.

Shah, N.S., Ali, J., Sayed, M., Ul, Z., Khan, H., Iqbal, J., Arshad, S., 2020. Synergistic effects of H_2O_2 and $S_2O_8^{2-}$ in the gamma radiation induced degradation of congo-red dye: kinetics and toxicities evaluation, Sep. Purif. Technol. 233:115966 https:// doi.org/10.1016/j.seppur.2019.115966.

Singh, P.; Quraishi, M. A. 2016. Corrosion Inhibition of Mild Steel Using Novel Bis Schiff's Bases as Corrosion Inhibitors: Electrochemical and Surface Measurement. Measurement 2016, 86, 114–124. DOI: 10.1016/j.measurement.2016.02.052.

Solmaz, R., 2014. Investigation of corrosion inhibition mechanism and stability of Vitamin B1 on mild steel in 0.5M HCl solution. Corrosion Science, 81:75-84

Swetha, G.A., Sachin, H.P., Guruprasad, A.M., Prasanna, B.M., Sudheer Kumar, K.H., 2018. Use of Seroquel as an effective corrosion inhibitor for low carbon steel in 1 M HCl. J. Bio. Tribo. Corrosion. 4 (2018) 57.

Ugwuja, C.G., Adelowo, O., Ogunlaja, A., Omorogie, M.O, Olukanni, O., Ikhimiukor, O., Iermak, I., Kolawole, G., Guenter, C., Taubert, A., 2019. Visible-light mediated photodynamic water disinfection@ bimetallic doped hybrid clay nanocomposites. ACS Appl Mater Interfaces 11(28): 25483–25494.

Vashi R. T. and Zele S. A., 2021. Green Corrosion Inhibitors for Zinc -An Overview. International Journal of Advances in Engineering and Management (IJAEM) Vol. 2, Issue 12, pp: 130-142.

Wadhwani, P.M., Panchal, V.K., Shah, N.K., 2015. Newly synthesized salicylidene-4,4′-dimorpholine (SDM) assembled on nickel oxide nanoparticles (NiONPs) and its inhibitive effect on mild steel in 2N hydrochloric acid. Applied Surface Science, 331:373-387.

Zhou, L., Ma, J., Zhang, H., Shao, Y., Li, Y., 2015. Fabrication of magnetic carbon composites from peanut shells and its application as a heterogeneous Fenton catalyst in removal of methylene blue. Appl. Surf. Sci. 324:490-498 https://doi.org/10.1016/j. apsusc.2014.10.152.